AIAA JOURNAL
Vol. 37, No. 1, January 1999

Rivulet Formation in Surface-Water Flow on an Airfoil in Rain

Brian E. Thompson* and Monica R. Marrochello†
Rensselaer Polytechnic Institute, Troy, New York 12180-3590

The location of the onset of rivulet formation in the surface-water flow over a wing with a NACA 4412 airfoil in rainfall rates of 50–160 mm/h is calculated and compared with wind-tunnel experiments. A model is presented in which rivulets form when the surface-tension shear stress between the liquid and the airfoil surface equals the interface shear stress caused by aerodynamic forces on the liquid due to air motion. Surface-tension shear stresses are obtained from measurements of surface tension and contact angle at the solid-water interface. Aerodynamic shear stresses are calculated by solution of Reynolds-averaged Navier–Stokes equations. Comparisons of calculated and measured locations of the onset of rivulet formation agreed within about 3% of chord for wettable and nonwettable surfaces at incidence up to stall for Reynolds numbers of 2.5×10^5 to 4×10^5.

Introduction

THE flow of water accumulated on the surface of an airfoil in rain affects aerodynamic performance and is influenced by surface tension, effective surface roughness, and aerodynamic forces. In rain at rates in the range of 50–160 mm/h, rivulets cause an increase in surface roughness for the aerodynamic boundary layer,[1] and both the structure and formation of rivulets depend on surface wettability.[2] Regions of surface-water flow have been identified on the suction side of an airfoil surface,[3,4] and the droplet-impact, film-convection, rivulet-formation, and droplet-convection regions have been defined.[4]

In the droplet-impingement region, rain impacts the leading edge and is either absorbed into the surface film or released back into the freestream as ejecta fog.[5,6] Droplet impacts increase the effective surface roughness experience by the airflow, which can cause boundary-layer transition prematurely and degrade aerodynamic performance.[1,2,7]

Downstream in the film-convection region, surface-water covers the airfoil surface like a transparent sheet and convects downstream driven by aerodynamic forces in a smooth, laminar film with some surface waves.[4] Farther downstream in the rivulet-formation region, instabilities that have grown in the surface-water flow cause the film to break up. The combined effects of surface tension and aerodynamic forces coalesce the film into individual, thin streams of water called rivulets that run chordwise toward the trailing edge. The flow rate and the direction of the rivulets are determined by aerodynamic shear forces acting at the free surface of the liquid.[4,5,8] Finally, in the droplet-convection region, surface tension forces cause the breakup of these rivulets into beads of water that convect individually toward the trailing edge where they coalesce into larger globules. Water is sheared away from the airfoil trailing edge by the external flow and is transported into the downstream wake.[2]

Aerodynamic force coefficients depend on the location of rivulet onset.[8] Measurements suggest that the greater the roughness of the rivulets and the greater the length of the region over which rivulets occur, the greater the drag and the smaller the lift.[8] Because of the influence of rivulet formation on airfoil performance, a method is presented in the next section to locate the onset of rivulet formation on airfoils, and this is followed by a section that presents calculations for the flow configuration of the experiments by Thompson et al.[4] and Thompson and Jang.[8] The penultimate section provides a brief discussion that compares measured and calculated locations of rivulet onset, and the paper closes with a summary of the salient conclusions.

Received March 17, 1998; revision received July 20, 1998; accepted for publication Sept. 24, 1998.

*Associate Professor, Department of Mechanical Engineering, Aeronautical Engineering, and Mechanics, RPI-MEAM-JEC 2049, 110 8th Street. Senior Member AIAA.

†Graduate Student, Department of Mechanical Engineering, Aeronautical Engineering, and Mechanics, RPI-MEAM-JEC 2049, 110 8th Street. Member AIAA.

Rivulet-Formation Model

Steady-state, theoretical analysis of rivulet formation in laminar and turbulent water sheets[9–11] is applied in the film-convection region to the surface flow of water that sheets over an airfoil in rain. The principle of the model is that rivulets form where the surface-tension shear stress, between the liquid and the wetted surface, is equal to the interface shear stress caused by aerodynamic forces on the liquid. At this location, the inertia of the surface-water flow is reduced such that the water surface contacts the airfoil surface and thereafter flows in channels, called rivulets, with essentially dry areas in between. This model defines a surface-tension skin friction that is obtained from physical properties of the liquid and the wetted surface and compares it with the aerodynamic skin friction obtained from computational fluid dynamics calculations of flow over dry airfoils. This section presents the model, and the next section compares calculated locations of rivulet onset with those measured[4,8] on a NACA 4412 airfoil in rain.

The restraining force due to surface tension at the solid-liquid interface[10] is given by

$$T_\sigma = \sigma(1 - \cos\theta) \tag{1}$$

where θ is the contact angle and σ is the surface tension. The contact angle is defined as the angle between the tangent to the liquid surface at the air-liquid-solid interface and the solid surface upon which the liquid rests.

The interface shear stress due to flow in the aerodynamic boundary layer is defined as

$$T_i = C_{f,c}\,\tfrac{1}{2}\rho_{\text{air}} U_\infty^2 \tag{2}$$

where $C_{f,c}$ is the aerodynamic skin-friction coefficient and U_∞ is the freestream velocity. The skin-friction coefficient causes the uniform liquid film to transition to an unstable water stream and to form rivulets. Rivulet formation occurs at the location where[10]

$$T_\sigma = T_i \tag{3}$$

Surface-Tension Skin Friction

The surface-tension shear stress is calculated from Eq. (1) using experimental values of the contact angle and the liquid-to-air surface tension. It is convenient to express this shear stress in the form of a skin-friction coefficient for comparison with the aerodynamic shear stresses described later. Combining the preceding three equations leads to the following definition of the surface-tension skin-friction coefficient:

$$C_{f,c} = \frac{2\sigma}{\rho_{\text{air}} U_\infty^2}(1 - \cos\theta) \tag{4}$$

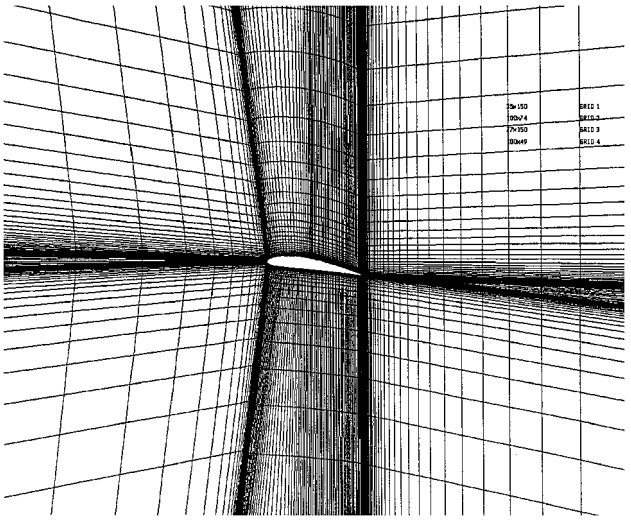

Fig. 1 Computational grid for a NACA 4412 airfoil at 8.0-deg incidence.

Aerodynamic Skin Friction

The shear stress due to aerodynamic forces at the boundary between the moving air and the surface-water film is modeled as that which would occur between the airflow and the stationary solid surface of a dry airfoil. This approximation follows from the experimental observations, first, that the surface velocity of the water film is small in the present experiments partly because gravitational forces are negligible on the nearly horizontal surface in this region and, second, that calculations showed that the present surface-water film is too thin to affect the pressure distribution around the airfoil or the local rate of boundary-layer development.

In contrast, the surface-water flow does affect the location of laminar-turbulence transition. In the present calculations, transition is fixed at the leading edge because of experimental evidence that shows there is cratering near the leading edge where droplets impact the surface water: This cratering effects a significant increase in surface roughness and stimulates turbulent aerodynamic flow.

The aerodynamic skin-friction coefficient was calculated by the solution of two-dimensional, Reynolds-averaged, Navier–Stokes equations in conservative form[12] using the linearized block implicit numerical procedure,[13,14] which employs centered spatial differences with adjustable numerical dissipation. Figure 1 shows the computational mesh generated for the experiments of Thompson et al.[4] and Thompson and Jang,[8] who tested a NACA 4412 airfoil section with blunt trailing-edge thickness of 0.0025 chord. The upper, lower, and exit boundaries were located 100 chord lengths from the airfoil. At the inflow boundary located 60 chords upstream of the airfoil, uniform flow was introduced. Elliptic equations were solved using the grid-generation routine EAGLE[15] to define the location of grid nodes between the airfoil surface and the boundaries. A mixing-length turbulence model was used because it is simple and provides reasonable accuracy.[12] Laminar-turbulence transition was fixed 0.8% chords downstream of the airfoil leading edge.

The calculated results that follow are subject to uncertainties that result from numerical, boundary-condition, and turbulence-model assumptions that are difficult to isolate. Numerical uncertainties in the present calculations were estimated using the grid convergence index GCI.[16–18] The GCI is calculated based on a generalized Richardson extrapolation and assumes that only ordered discretized errors exist in the solution.[17] It is assumed that the solution for finer grids approaches the exact solution and that the error approaches zero in the limit of the grid spacing approaching zero.[18] For the present calculations, the CGI was calculated using converged solutions on grids of 185×125 and 210×150 nodes. The differences in the aerodynamic coefficients of lift, drag, and moment were less than 1.4, 5.8, and 2.8%, respectively. The difference in the drag coefficient obtained with each grid is greater than that in the lift, confirming again that calculated drag is more sensitive than lift to numerical approximations. The differences in the CGI and aerodynamic performance reflect a grid dependence that is adjudged to be acceptable for the present engineering purposes following the recommendations of Lotz et al.[16]

The aerodynamic skin-friction coefficient was obtained from the following expression:

$$C_f = \frac{\tau_w}{\frac{1}{2}\rho_{\text{air}} U_\infty^2} \tag{5}$$

in which the wall shear stress τ_w was obtained from the linear distribution of mean velocity calculated below y^+ of 5 in the aerodynamic boundary layer. The location of rivulet onset is identified as where this aerodynamic skin-friction coefficient equals the surface-tension skin-friction coefficient of Eq. (4).

Results

Measured and calculated results were obtained for a NACA 4412 airfoil in subsonic flight in the Reynolds-number range of 1×10^5 to 4×10^5 and in rainfall rates of 50–150 mm/h. The experimental results[8] showed that flow was two dimensional over more than 80% of chord at incidence of about -2 to 12 deg, and accordingly calculations were limited to this range. Results are compared on a wettable surface that was a sunlight curable epoxy with a measured contact angle of 64 deg, and a nonwettable surface that was a silicon coating with a measured contact angle of 120 deg. The water-to-air interface surface tension was measured to be 58 dyne/cm.[8] With these measured values in Eq. (4), the surface-tension skin-friction coefficients are 0.00832 and 0.0111 for the wettable and nonwettable coatings, respectively.

Figures 2–4 show calculated distributions of aerodynamic skin-friction coefficient at low, moderate, and large angles of attack, respectively. Calculated and measured locations of rivulet onset for wettable and nonwettable surfaces are also shown in Fig. 2. Measured locations of rivulet onset were obtained from photographs of the NACA 4412 airfoil suction side taken during wind-tunnel tests to within an experimental uncertainty of about 1% of chord. For example, at a Reynolds number of 2.5×10^5 and an incidence of 8.0 deg, the locations of the onset of rivulet formation were calculated to be at x/c of 0.264 and 0.104 and were measured at about 0.25 and 0.10 for the wettable epoxy and nonwettable silicon, respectively.

Figures 5 and 6 show measured and calculated locations of the onset of rivulet formation for wettable and nonwettable surfaces, respectively. Calculated results were not obtained for angles of attack greater than 12.0 deg because experiments show that flow over the airfoil has large regions with significant crossflow and vortical structures.

Discussion

The present calculations provide insights into the flow structure around airfoils in rain. Velocity distributions at angles of attack between -2 and 12 deg show that the boundary layers remain attached throughout the droplet-impact, film-convection, and rivulet-formation regions. Calculated values of lift and drag coefficients agree within 2 and 6%, respectively, of measurements,[19,20] which justifies, in part, the choice of a mixing-length turbulence model and the chosen location of far-field boundaries. More specifically at an incidence of 8 deg and a Reynolds number of 2.5×10^5, the calculated lift and drag coefficients are 1.27 and 0.0204, respectively, and compare with experimental values[19] of 1.23 and 0.0198, respectively, which is consistent with previous observations that viscous effects are more important to lift than to drag.[21]

Calculated locations of rivulet onset are consistent with trends[8] in the measurements. Specifically, the onset of rivulet formation occurs closer to the leading edge on nonwettable surfaces than on wettable surfaces, and the onset of rivulet formation moves farther downstream with decreasing Reynolds number. Measured and calculated locations of rivulet onset are sensibly within about 2% of chord for the wettable surface and about 3% of chord for the nonwettable surface in the range of incidence from 5 to 12 deg, although agreement is poorer at lower incidence as discussed later. The distributions of aerodynamic skin-friction coefficients at incidence of 5–12 deg

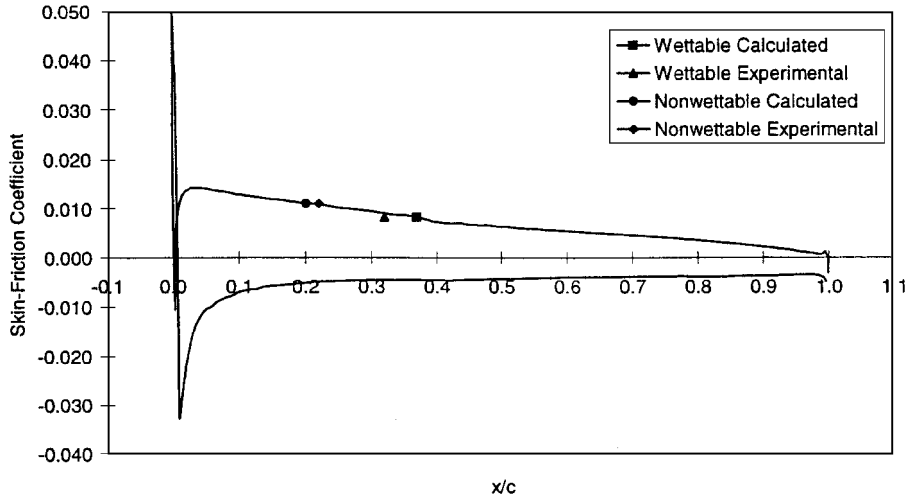

Fig. 2 Calculated aerodynamic skin-friction coefficient on a NACA 4412 airfoil at an angle of attack of −2 deg and Reynolds number of 1×10^5.

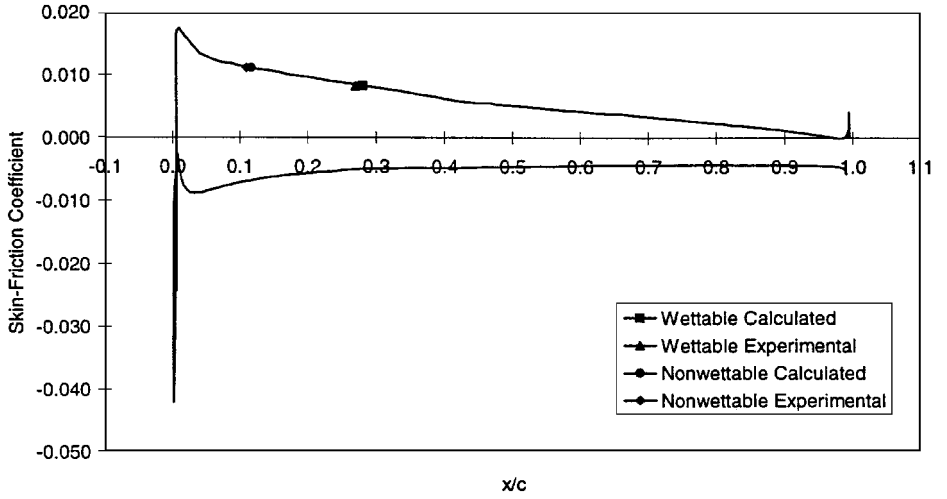

Fig. 3 Calculated aerodynamic skin-friction coefficient on a NACA 4412 airfoil at an angle of attack of 6 deg and Reynolds number of 2.5×10^5.

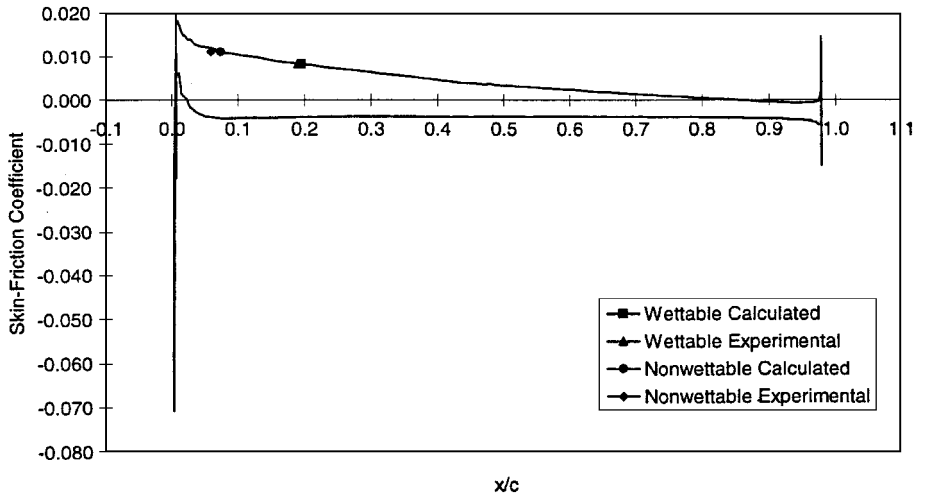

Fig. 4 Calculated aerodynamic skin-friction coefficient on a NACA 4412 airfoil at an angle of attack of 12 deg and Reynolds number of 4×10^5.

show clear peaks near the leading edge, such as those apparent on Figs. 3 and 4, and so uncertainty in the surface-tension shear stress has a negligible effect on the predicted location of rivulet onset.

At angles of incidence from −2 through 4 deg, distributions of suction-side skin-friction coefficients do not display pronounced large, sharp peaks but instead have rounded peaks just downstream of the leading edge similar to the peak shown in Fig. 2. An uncertainty of 1% in surface-tension shear stress translates into a movement of 10, 4, and 2% of chord at −2, 0, and 4 deg because the value of the skin-friction coefficient becomes more nearly constant immediately downstream of the suction peak as the incidence decreases. This extreme sensitivity to uncertainty in the measurement of surface-tension shear stress accounts for the increasingly poorer and poorer agreement between calculated and measured values of the onset of rivulet formation below angles of attack of 4 deg at Reynolds numbers between 2.5×10^5 and 4×10^5.

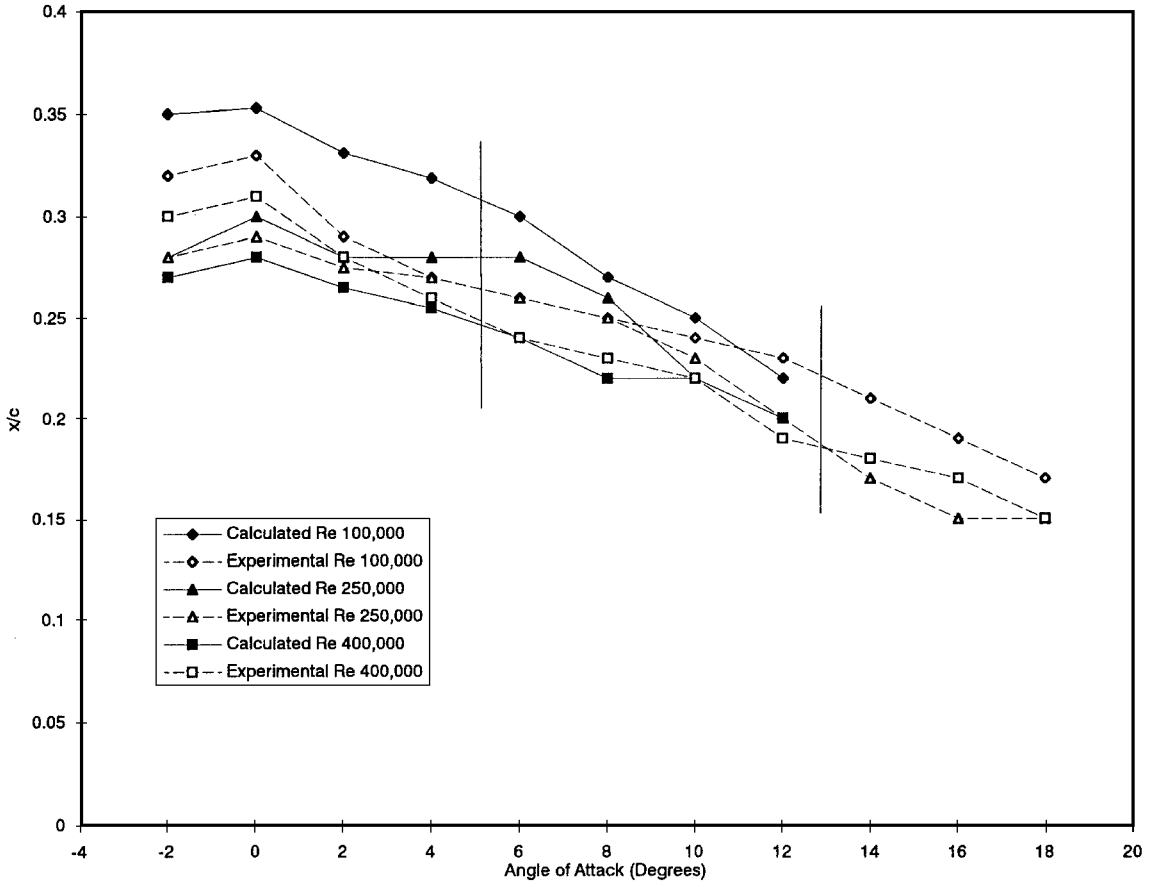

Fig. 5 Locations of the onset of rivulet formation on the wettable surface of the NACA 4412 airfoil in rain rates of 50–150 mm/h.

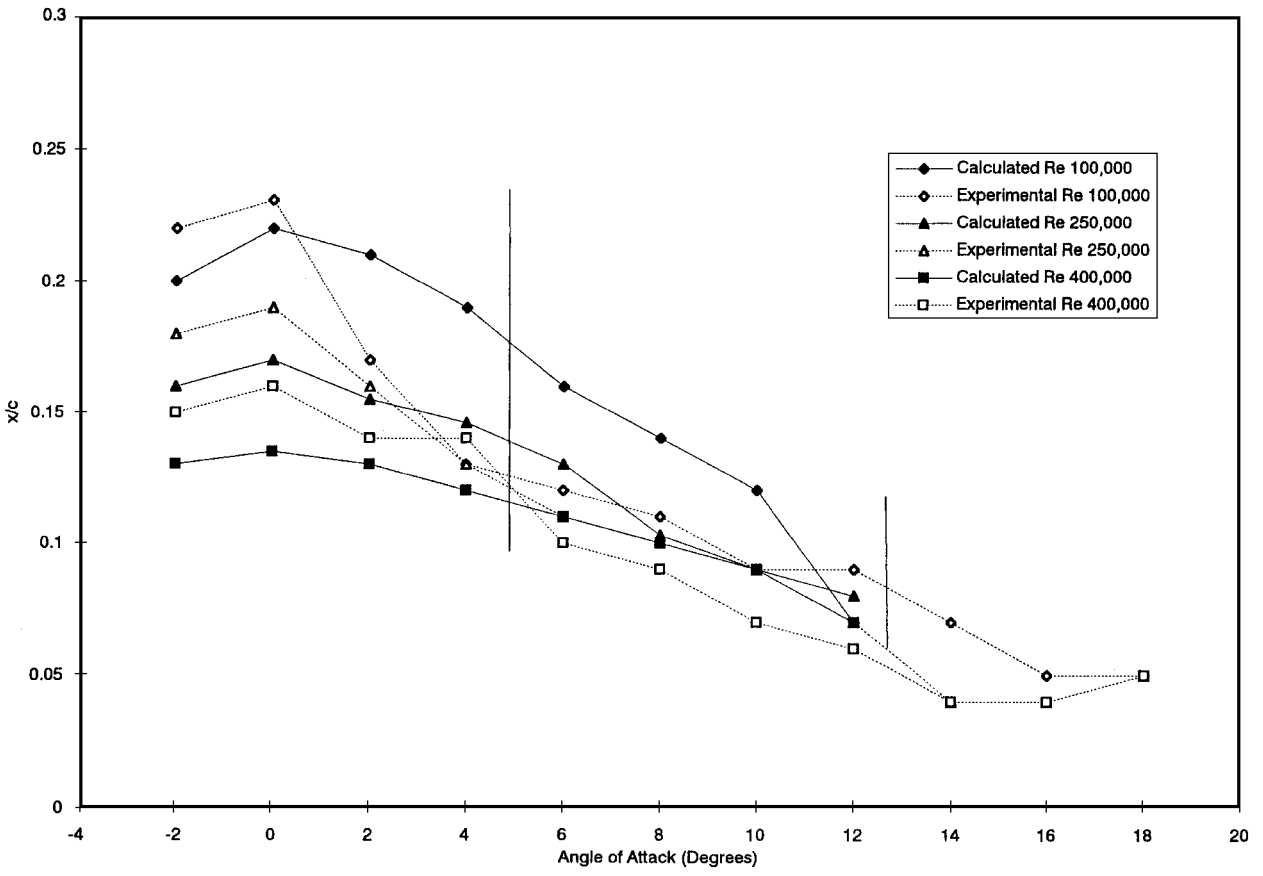

Fig. 6 Locations of the onset of rivulet formation on the nonwettable surface of the NACA 4412 airfoil in rain rates of 50–150 mm/h.

In contrast, the locations of rivulet formation at Reynolds numbers of 1×10^5 are about 4% of chord too far downstream for all angles of attack. This corresponds to an underprediction of about 0.001 in the calculated value of the skin-friction coefficient: a value that is almost constant over the entire incidence range. The present model represents additional turbulence production associated with cratering and reabsorption of the ejecta fog in the droplet-impact region only by fixing transition near the leading edge. Such a systematic underprediction of aerodynamic skin friction suggests that at Reynolds numbers below about 1×10^5 turbulence production immediately downstream of transition may have a significant component due to rain effects in the droplet-impact region, in addition to that caused by shear forces in the aerodynamic boundary layer, and the former is neglected in the present model.

Concluding Remarks

Calculated and measured values of the location of the onset of rivulet formation are compared on the suction-side surface of an airfoil in low-speed flight at incidence up to stall in rainfall at rates of 50–160 mm/h. The location of the onset of rivulet formation was calculated within 3% of chord of experimental values with a method that applied the following assumptions: 1) rivulet onset was identified at the location where the aerodynamic shear stress equals the surface-tension shear stress, 2) the only significant effect of the surface-water flow was to cause early transition in the droplet-impact region, and 3) the film of surface-water flow was so thin that it did not influence the pressure distribution or local boundary-layer development.

References

[1]Marchman, J. F., III, Robertson, E. A., and Emsley, H. T., "Rain Effects at Low Reynolds Number," *Journal of Aircraft*, Vol. 24, No. 9, 1987, pp. 638–644.

[2]Hansman, R. J., and Barsotti, M. F., "The Aerodynamic Effect of Surface Wetting Characteristics on a Laminar Flow Airfoil in Simulated Heavy Rain," AIAA Paper 85-0260, Jan. 1985.

[3]Al-Khalil, K. M., Keith, T. G., and De Witt, K. J., "Development of an Anti-Icing Runback Model," AIAA Paper 90-0759, Jan. 1990.

[4]Thompson, B. E., Jang, J., and Dion, J. L., "Wing Performance in Moderate Rain," *Journal of Aircraft*, Vol. 32, No. 5, 1995, pp. 1034–1039.

[5]Bezos, G. M., Dunham, R. E., Jr., Gentry, G. L., Jr., and Melson, W. E., Jr., "Wind Tunnel Aerodynamic Characteristics of a Transport-Type Airfoil in a Simulated Heavy Rain Environment," NASA TP 3184, 1992.

[6]Bilanin, A. J., "Scaling Laws for Testing of High Lift Airfoils Under Heavy Rainfall," AIAA Paper 85-0257, 1985.

[7]Haines, P. A., and Luers, J. K., "Aerodynamic Penalties of Heavy Rain on a Landing Aircraft," NASA CR-156885, 1982.

[8]Thompson, B. E., and Jang, J., "Aerodynamic Efficiency of Wings in Rain," *Journal of Aircraft*, Vol. 33, No. 6, 1996, pp. 1047–1053.

[9]Duckler, A. E., and Bergelin, O. P., "Characteristics of Flow in Falling Liquid Films," *Chemical Engineering Progress*, Vol. 48, No. 11, 1952, pp. 557–563.

[10]Hartley, D. E., and Murgatroyd, W., "Criteria for the Break-up of Thin Liquid Layers Flowing Isothermally over Solid Surfaces," *International Journal of Heat and Mass Transfer*, Vol. 7, No. 9, 1964, pp. 1003–1015.

[11]Towell, G. D., and Rothfeld, L. B., "Hydrodynamics of Rivulet Flow," *AIChE Journal*, Vol. 12, No. 5, 1966, pp. 972–980.

[12]Thompson, B. E., and Lotz, R. D., "Transonic Flow Around Divergent Trailing-Edge Airfoils," *Journal of Aircraft*, Vol. 33, No. 5, 1996, pp. 950–955.

[13]Briley, W. R., and McDonald, H., "Solution of the Multi-Dimensional Compressible Navier–Stokes Equations by a Generalized Implicit Method," *Journal of Computational Physics*, Vol. 24, No. 4, 1977, pp. 372–397.

[14]Briley, W. R., and McDonald, H., "On the Structure and Use of Linearized Block Implicit Schemes," *Journal of Computational Physics*, Vol. 34, No. 1, 1980, pp. 54–73.

[15]Thompson, J. F., *EAGLE User Manual 1988*, Engineering Research Center for Computational Field Simulation, Mississippi State Univ., Mississippi State, MS, 1988.

[16]Lotz, R. D., Thompson, B. E., Konings, C. A., and Davoudzadeh, F., "Numerical Uncertainties in Transonic Flow Calculations for Airfoils with Blunt Trailing Edges," *International Journal for Numerical Methods in Fluids*, Vol. 24, No. 4, 1997, pp. 355–373.

[17]Roache, P. J., "A Method for Uniform Reporting of Grid Refinement Studies," *Quantification of Uncertainty in Computational Fluid Dynamics*, edited by I. Celik, C. J. Chen, P. J. Roach, and G. Scheurer, ASME FED-Vol. 158, American Society of Mechanical Engineers Fluids Engineering Div. Summer Meeting, Washington, DC, June 1993.

[18]Roache, P. J., "Perspective: A Method for Uniform Reporting of Grid Refinement Studies," *Journal of Fluids Engineering*, Vol. 116, No. 3, 1994, pp. 405–413.

[19]Abbott, I. H., and von Doenhoff, E., *Theory of Wing Sections*, 2nd ed., Dover, New York, 1959.

[20]Jang, J., "Aerodynamic Performance of Wings in Rain," Ph.D. Thesis, Dept. of Mechanical Engineering, Aeronautical Engineering and Mechanics, Rensselaer Polytechnic Inst., Troy, NY, 1995.

[21]Thompson, B. E., and Whitelaw, J. H., "Trailing-Edge Region of Airfoils," *Journal of Aircraft*, Vol. 26, No. 3, 1989, pp. 225–234.

J. P. Gore
Associate Editor